Cell Metabolism
Article

Glucagon-Induced Acetylation of Foxa2 Regulates Hepatic Lipid Metabolism

Ferdinand von Meyenn,[1,2,5] Thomas Porstmann,[1,2,5] Emanuel Gasser,[1,2] Nathalie Selevsek,[3] Alexander Schmidt,[4] Ruedi Aebersold,[2,3] and Markus Stoffel[1,2,*]
[1]Institute of Molecular Health Sciences
[2]Competence Center for Systems Physiology and Metabolic Diseases
ETH Zurich, Schafmattstrasse 22, 8093 Zurich, Switzerland
[3]Institute of Molecular Systems Biology, ETH Zurich, Wolfgang-Pauli Strasse 16, 8093 Zurich, Switzerland
[4]Proteomics Core Facility, Biozentrum, University of Basel, Klingelbergstrasse 50/70, 4056 Basel, Switzerland
[5]These authors contributed equally to this work
*Correspondence: stoffel@biol.ethz.ch
http://dx.doi.org/10.1016/j.cmet.2013.01.014

SUMMARY

Circulating levels of insulin and glucagon reflect the nutritional state of animals and elicit regulatory responses in the liver that maintain glucose and lipid homeostasis. The transcription factor Foxa2 activates lipid metabolism and ketogenesis during fasting and is inhibited via insulin-PI3K-Akt signaling-mediated phosphorylation at Thr156 and nuclear exclusion. Here we show that, in addition, Foxa2 is acetylated at the conserved residue Lys259 following inhibition of histone deacetylases (HDACs) class I–III and the cofactors p300 and SirT1 are involved in Foxa2 acetylation and deacetylation, respectively. Physiologically, fasting states and glucagon stimulation are sufficient to induce Foxa2 acetylation. Introduction of the acetylation-mimicking (K259Q) or -deficient (K259R) mutations promotes or inhibits Foxa2 activity, respectively, and adenoviral expression of Foxa2-K259Q augments expression of genes involved in fatty acid oxidation and ketogenesis. Our study reveals a molecular mechanism by which glucagon signaling activates a fasting response through acetylation of Foxa2.

INTRODUCTION

Mammals have evolved complex mechanisms to maintain energy homeostasis during periods of nutritional abundance and starvation. The nutritional state of an organism is reflected by the circulating levels of the two pancreatic hormones insulin and glucagon, which elicit regulatory responses in the peripheral tissues as a means of maintaining glucose and lipid homeostasis. In particular, the liver acts as a "metabolic integrator," by regulating glycogen degradation, gluconeogenesis, fatty acid oxidation, and ketogenesis, thereby maintaining normoglycemia and ensuring constant energy supply to glucose-dependent tissues such as the brain.

Following food intake, plasma insulin levels rise and suppress hepatic glucose production, β-oxidation, and ketogenesis and instruct the liver to convert glucose to glycogen for storage—a process regulated by the insulin-sensitive enzyme glycogen synthase kinase-3—and promote triglyceride (TG) synthesis as well as de novo lipogenesis (Kahn et al., 2006). Many metabolic responses are elicited by changes in plasma insulin levels that are mediated by the insulin/PI3K/Akt signaling cascade. Downstream targets of the Akt kinases are the tuberous sclerosis 1 (Tsc1)-Tsc2 complex, glycogen synthase kinase 3 (GSK3), and several members of the forkhead box transcription factors (Saltiel and Kahn, 2001), such as Foxo1, which plays a central role in hepatic glucose metabolism (Lin and Accili, 2011), and Foxa2, a key regulator of hepatic lipid metabolism. The forkhead member Foxa2, which is transcriptionally active in the fasted state and induces expression of enzymes involved in fatty acid oxidation, ketogenesis, and VLDL secretion and bile acid metabolism (Wolfrum et al., 2004; Wolfrum and Stoffel, 2006; Bochkis et al., 2008), is regulated via insulin/PI3K/Akt-mediated phosphorylation at a single conserved threonine (Thr156) residue (Wolfrum et al., 2003). This phosphorylation event attenuates Foxa2 activity and triggers nuclear export in a CRM1-dependent manner (Wolfrum et al., 2003, 2004; Howell and Stoffel, 2009; Pandey et al., 2009; Banerjee et al., 2010). Interestingly, insulin inhibits the transcriptional activity of Foxa2 in the liver not only during feeding, but also in hyperinsulinemic *ob/ob* or *db/db* mice and in animals with diet-induced obesity. Expression of constitutively active Foxa2-T156A in diabetic mice normalizes plasma glucose levels, decreases hepatic triglyceride content, increases insulin sensitivity, and elevates hepatic lipid metabolism by activating the expression of genes encoding enzymes involved in mitochondrial β-oxidation and ketogenesis, such as CPT1α, MCAD, VLCAD, or HMGCS (Wolfrum et al., 2004; Wolfrum and Stoffel, 2006).

During starvation or hypoglycemia, high glucagon concentrations induce glycogen breakdown and gluconeogenesis in the liver in order to release glucose into the circulation (Habegger et al., 2010). Glucagon also stimulates hepatic mitochondrial β-oxidation to supply energy for glucose production and conversion of fatty acids into ketone bodies, which can provide up to two-thirds of the energy for the brain in periods of glucose shortage. At the molecular level, binding of glucagon to its receptor causes activation of a heterotrimeric, stimulatory G protein (G_S), which subsequently leads to interaction and stimulation of adenylate cyclase and elevation of cAMP levels and

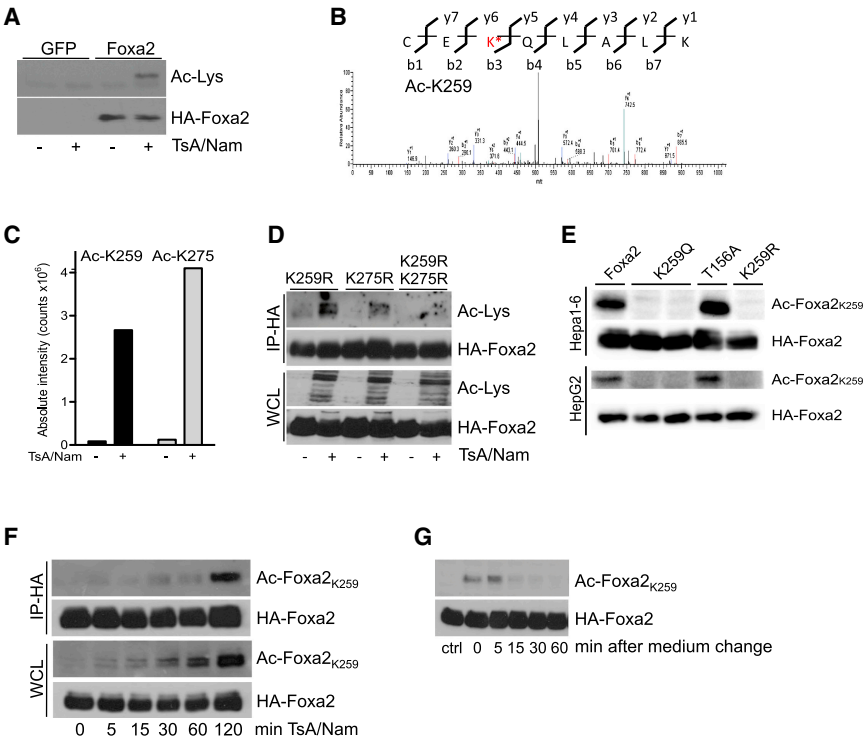

Figure 1. Lys259 Is Acetylated in Foxa2

(A) Hepa1-6 cells were infected with recombinant adenovirus expressing HA-tagged Foxa2 prior to overnight serum starvation and treated with 5 mM Nam and 2 μM TsA for 2 hr. Foxa2-HA was immunoprecipitated using an anti-HA antibody, and acetylated Foxa2 was detected using a global acetylated lysine antibody.

(B) Samples under (A) were further processed for MS analysis. Tandem MS analyses of acetylated Foxa2 are shown that identify Lys259 (K* corresponds to the acetylated lysine).

(C) Absolute intensities of the peptides containing Ac-Lys259 (black) and Ac-Lys275 (gray) obtained by MS analysis after addition of the inhibitor TsA/Nam to Hepa1-6 cells.

(D) Hepa1-6 cells were infected with the indicated recombinant adenovirus expressing HA-tagged Foxa2 and treated as indicated. Immunoblots of whole lysis and precipitates were probed with antibodies against HA and acetylated lysine.

(E) Hepa1-6 and HepG2 were infected with the indicated recombinant adenovirus expressing HA-tagged Foxa2 and treated with TsA/Nam for 2 hr. Immunoblots of precipitates were probed with antibodies against HA and acetylated Foxa2 Lys259.

(F) Hepa1-6 cells were treated with TsA/Nam for the indicated time, and acetylated Foxa2 Lys259 was detected by western analysis.

(G) Hepa1-6 cells, cultured in full medium, were treated with TsA/Nam for 2 hr and subsequently washed and incubated in full medium lacking TsA/Nam for the indicated time. Acetylated Foxa2 Lys259 was detected by western analysis. Ctrl: non-inhibitor-treated cells.

activation of cAMP response element-binding protein (CREB)-regulated transcription coactivator 2 (CRTC2; TORC2) and protein kinase A (PKA) (Habegger et al., 2010). A target of active PKA is CREB, which upon phosphorylation translocates into the nucleus and promotes expression of gluconeogenic genes, such as pyruvate carboxylase, PEPCK1, or G6PC (Altarejos and Montminy, 2011) or salt-inducible kinase 2 (SIK2), an inhibitor of CRTC2 (Koo et al., 2005). CRTC2 activity is also regulated by CBP/p300-mediated acetylation, and p300 activity is suppressed by phosphorylation via SIK2 (Liu et al., 2008).

In this study, we tested the hypothesis that PTMs other than phosphorylation regulate the activity of Foxa2. Our unbiased analysis of posttranslational modifications of Foxa2 revealed an evolutionarily conserved and regulated acetylation site that modulates the transcriptional activity and hepatic lipid metabolism in response to fasting and glucagon stimulation.

RESULTS

Foxa2 Is Acetylated at Lys259 and Lys275

To investigate whether Foxa2 is modified by acetylation, we expressed recombinant HA-tagged wild-type Foxa2 in the mouse liver cell line Hepa1-6 using an adenovirus and treated the cells with an histone deacetylase (HDAC) inhibitor cocktail containing trichostatin A (TsA) and nicotinamide (Nam). After immunoprecipitation of Foxa2, we could detect acetylated Foxa2 in the presence of the inhibitor cocktail using an anti-acetyl-lysine antibody (Figure 1A). Tandem mass spectrometry (MS) analysis of affinity-purified HA-Foxa2, expressed in liver cells in the presence of HDAC inhibitors, identified two specific acetylation sites, namely Lys259 and Lys275 (Figures 1B and S1A). We found both sites acetylated upon HDAC inhibition (Figure 1C). To confirm these results, we generated recombinant adenoviruses expressing acetylation-deficient Foxa2 by mutating Lys259 and Lys275 to arginine (K259R and K275R, respectively). When cells were infected with the single mutants K259R or K275R, acetylated lysine was still detectable, whereas double mutant Foxa2 (K259R-K275R) profoundly diminished the effect of the inhibitor cocktail on Foxa2 acetyl-lysine (Figure 1D). These results indicate that Lys259 and Lys275 are the two principal lysine residues acetylated in the presence of the HDAC inhibitors in the liver cell line Hepa1-6. We were also able to detect acetylation of Foxa2 Lys259, but not Foxa2 Lys275, in the human liver cell line HepG2 by MS analysis (Figure S1B).

Since Foxa2 Lys259 is highly conserved in vertebrates as well as within the FoxA subfamily (Figure S1C) and is localized at the junction of the nuclear localization sequence (NLS) and the DNA binding domain (Howell and Stoffel, 2009), we decided to study the biological function of acetyl-Lys259. We generated a specific anti-Foxa2-Ac-Lys259 antibody, which recognizes acetylated Foxa2 in mouse Hepa1-6 cells, as well as in human HepG2 cells (Figure 1E). Accumulation of acetyl-Lys259 can be detected within 2 hr of HDAC inhibitor treatment in whole-cell lysates and immunoprecipitated Foxa2 (Figure 1F), and Lys259 is rapidly deacetylated after HDAC inhibitor removal (Figure 1G), with acetyl-Lys259 being detectable 5 min after medium replacement and markedly diminished after 15 min. Similar

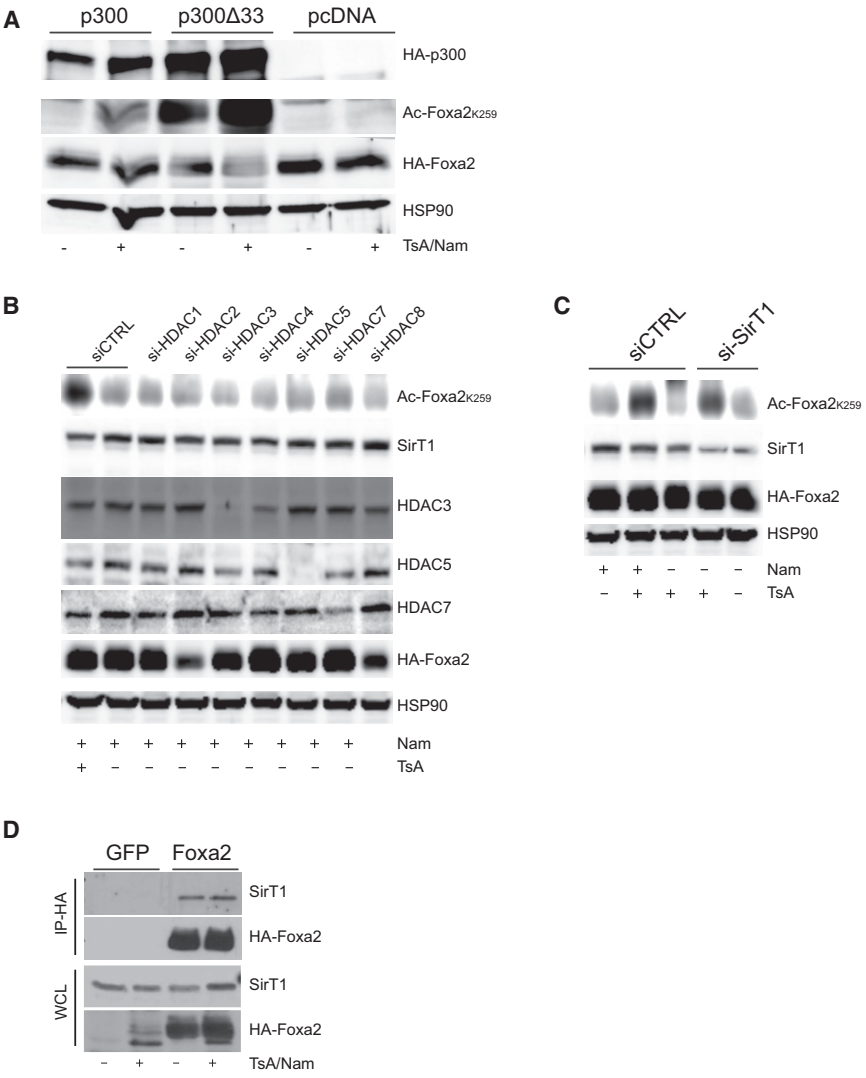

Figure 2. Foxa2 Lys259 Is Acetylated by HAT p300 and Deacetylated by HDACs of Class I/II and Sirt1

(A) Primary hepatocytes from *C57BL/6* mice were transfected with expression vectors containing Foxa2 in combination with the indicated KAT constructs. Forty-eight hours posttransfection, cells were treated with 2 μM TsA and 5 mM Nam for 2 hr, and Foxa2-HA were immunoprecipitated using anti-HA antibodies. Acetylated Lys259 in Foxa2 were detected using an acetylated Foxa2 Lys259 specific antibody.

(B and C) Hepa1-6 were transfected with expression vectors containing Foxa2 in combination with siRNAs against the indicated HDACs. Forty-eight hours posttransfection, cells were treated with 2 μM TsA or 5 mM Nam for 2 hr, and acetylated Lys259 in Foxa2 were assessed by western analysis. siRNA sequences are shown in Table S1.

(D) Hepa1-6 cells were infected with recombinant adenovirus expressing HA-tagged Foxa2 constructs as indicated and treated with TsA/Nam for 2 hr. Immunoblots of whole-cell lysis and immunoprecipitates (IP-HA) were probed for endogenous Sirt1 and HA-tagged Foxa2.

results were obtained by replacing the media with starvation medium without FBS (data not shown). These results indicate that acetylation at Lys259 in Foxa2 is a highly dynamic and reversible process.

Sirt1 and p300 Regulate Acetylation of Foxa2

Acetylation is regulated by two groups of enzymes, lysine-acetyltransferases (KATs) and HDACs. KATs are divided into two main categories, KAT A and KAT B, which can be further classified into subclasses. CBP/p300, PCAF, GCN5, Tip60, and SRC1 are representative members. To identify the KAT that acetylates Foxa2 at Lys259, we cotransfected HA-tagged Foxa2 with at least one KAT of each subclass. After 48 hr cells were treated with TsA/Nam and levels of acetyl-Lys259 were measured (Figures 2A, S2A, and S2B). Overexpression of p300 alone is sufficient to detect acetyl-Lys259, which can be further increased with HDAC inhibitor treatment. The constitutively active KAT p300Δ33 enhanced the acetyl-Lys259 signal compared to wild-type p300 on HA-tagged Foxa2 and also resulted in acetylation of endogenous Foxa2 (Figure S2C). Knockdown of p300 by RNAi decreased the TsA/Nam-induced acetyl-Lys259 signal (Figure S2D). Consistent with this, pharmacological inhibition of p300 markedly reduced the induction of acetyl-Lys259 by TsA/Nam (Figure S2E). These data demonstrate that p300 is responsible for acetylating Foxa2 Lys259.

We next used a genetic and a pharmacological approach to identify the HDACs responsible for deacetylating Foxa2 Lys259. Cells were transfected with siRNAs targeting HDACs of class I/II or class III (sirtuins) and 48 hr later treated for 2 hr with the class III inhibitor Nam or with the class I/II inhibitor TsA, respectively (Figures 2B, 2C, and S2F). Knockdown of HDACs of class I/II in the presence of Nam did not result in increased acetyl-Lys259 levels, whereas knockdown of Sirt1 in combination with TsA led to increased acetylation of Foxa2 Lys259. In the complementary pharmacological approach, inhibition of a single class of HDAC using TsA for class I/II or Nam for class III did not enrich for acetyl-Lys259 (Figure S2G). Consistent with the result from the siRNA-mediated knockdown of HDACs, only inhibition of class I/II HDACs in combination with class III HDAC inhibitor TsA or the specific Sirt1 inhibitor Ex527 led to increased acetylation of Foxa2 Lys259. To confirm the role of Sirt1 as a Foxa2 deacetylase, we infected primary hepatocytes from wild-type or liver-specific Sirt1 knockout mice ($Sirt1^{fl/fl}$ × AlbCre) mice with recombinant adenovirus expressing HA-tagged Foxa2 prior to overnight starvation (Figure S2H). Acetylation of Foxa2 Lys259 was detected in primary hepatocytes in the absence of Sirt1.

In order to explore whether Foxa2 physically interacts with p300 and Sirt1, Hepa1-6 cells were infected with adenovirus

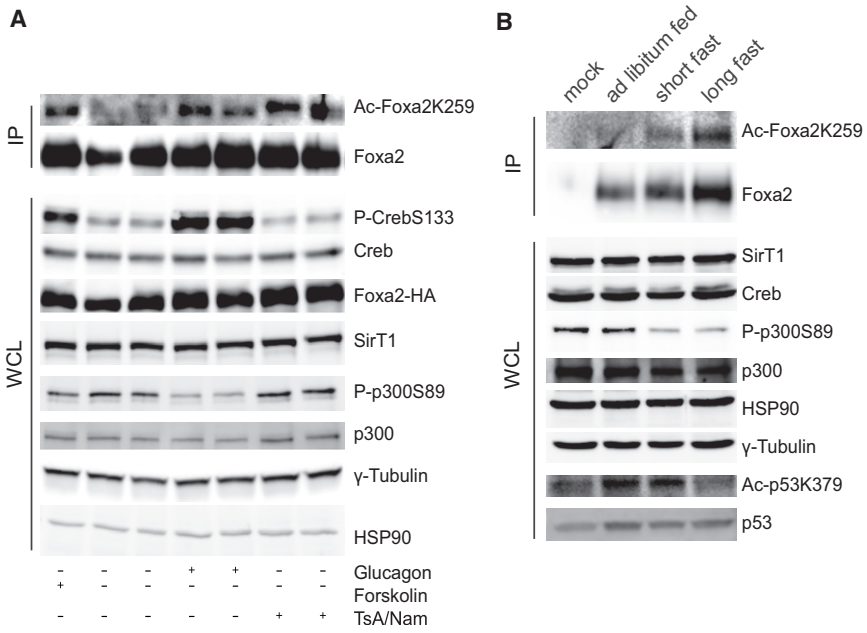

Figure 3. Hepatic Foxa2 Lys259 Is Acetylated in Response to Glucagon

(A) Primary hepatocytes from *C57BL/6* mice were infected with recombinant adenovirus expressing HA-tagged Foxa2 prior to overnight fasting and then treated with glucagon (0.5 μg/ml) or forskolin (10 μM) for 30 min. Acetylated Foxa2 Lys259 was detected in Foxa2-HA immunoprecipitates.

(B) *C57BL/6* mice were injected with recombinant adenovirus expressing HA-tagged Foxa2 and analyzed in ad libitum fed state or after a 14 or 24 hr fast. Acetylated Foxa2 Lys259 in the livers of fasted animals was detected in Foxa2-HA immunoprecipitates.

expressing HA-tagged Foxa2. Immunoprecipitation with anti-HA antibodies showed that Foxa2 was able to pull down endogenous Sirt1, independent of whether the cells were treated with TsA/Nam or not (Figure 2D). We also tested if Lys259 acetylation-mimicking (K259Q) or acetylation-deficient mutants (K259R) interact with Sirt1 and p300 by expressing Foxa2 K259Q or K259R in Hepa1-6 cells. The K259Q and the K259R mutants were able to coimmunoprecipitate endogenous Sirt1 and endogenous p300 (Figure S2I). These experiments show that Foxa2 can interact with Sirt1 and p300.

Foxa2 K259 Is Acetylated upon Fasting or Glucagon Stimulation

To identify physiological triggers for Foxa2-Lys259 acetylation, we isolated primary hepatocytes from wild-type mice; challenged them with several stimuli including metformin, AICAR, rapamycin, tunicamycin, cisplatin, etoposide, UV light, H_2O_2, heat shock, palmitate, insulin, glucagon, and forskolin; and analyzed the cell extracts for acetylated Lys259 (data not shown). Only upon stimulation with the pancreatic hormone glucagon could we detect an increase in the levels of acetylated Lys259, independent of HDAC inhibition (Figure 3A). In addition, forskolin, a commonly used drug to raise levels of cyclic AMP (cAMP), which are also raised in response to glucagon stimulation, was also able to increase Foxa2 Lys259 acetylation in primary hepatocytes. Downstream targets of the glucagon signaling pathway such as P-Creb were also activated in response to glucagon or forskolin treatment. We also detected a reduction of the inhibitory Ser89 phosporyaltion of p300 (Liu et al., 2008) in the glucagon-treated samples. Since glucagon levels are increased in the fasted state, opposing the actions of insulin, we sought to verify whether Foxa2 Lys259 acetylation was also regulated in vivo in response to fasting. We expressed HA-tagged wild-type Foxa2 in livers of lean mice using recombinant adenovirus and starved these animals. Whereas we did not detect Lys259 acetylation in ad libitum fed mice, acetylation levels increased after short starvation and even more after a long starvation period (Figure 3B). In agreement with the in vitro results, levels of Ser89 phosporyaltion of p300 were also reduced in the starved animals, and p53 Lys379 acetylation, a direct target of Sirt1, decreased with starvation. To summarize, Foxa2 Lys259 acetylation was increased upon glucagon stimulation in vitro and upon starvation in vivo.

Acetylation of Foxa2 Modulates Its Localization and Activity

Foxa2 shuttles from the nucleus to the cytoplasm in response to insulin signaling (Wolfrum et al., 2003). Since Lys259 resided at the junction of the NLS, we investigated whether acetylation influences intracellular localization of Foxa2. Treatment of Hepa1-6 cells with TsA and Nam blocked insulin-dependent nuclear exclusion of endogenous Foxa2 without affecting insulin signaling (Figures 4A and S3A). To further elucidate if Lys259 is responsible for localization of Foxa2 in vivo, we injected adenovirus expressing wild-type, K259Q, or K259R constructs or the nuclear and constitutively active T156A mutant into wild-type mice. Both endogenous and exogenous wild-type Foxa2 were located in the nucleus in all fasted animals (Figures 4B and 4C). As previously reported, hepatic Foxa2 was excluded from the nucleus of ad libitum fed animals, whereas the phosphorylation-deficient mutant T156A remained nuclear. Interestingly, the acetyl-deficient K259R mutant was mainly cytoplasmic in the fasted state, whereas the acetyl-mimic K259Q mutant remained in the nucleus in the fed state. We previously reported that the phospho-deficient T156A remains nuclear even in the presence of insulin signaling and is transcriptionally active. In order to investigate how the modifications affect one another, we combined acetylation mutations with T156A that inhibits Akt-mediated phosphorylation. Interestingly, the double T156A-K259R mutant was localized mainly to the cytosol, thereby behaving almost like the single K259R mutant.

In order to test if the nuclear localization of Foxa2 correlates with increased transcriptional activity, we analyzed acetylation-deficient and -mimic Foxa2 Lys259 mutants in livers of fed wild-type mice that were injected with adenovirus expressing the indicated Foxa2 mutants. The hepatic expression levels of all HA-tagged mutants were similar (Figure 4D). Transcript levels of known Foxa2 target genes encoding enzymes involved

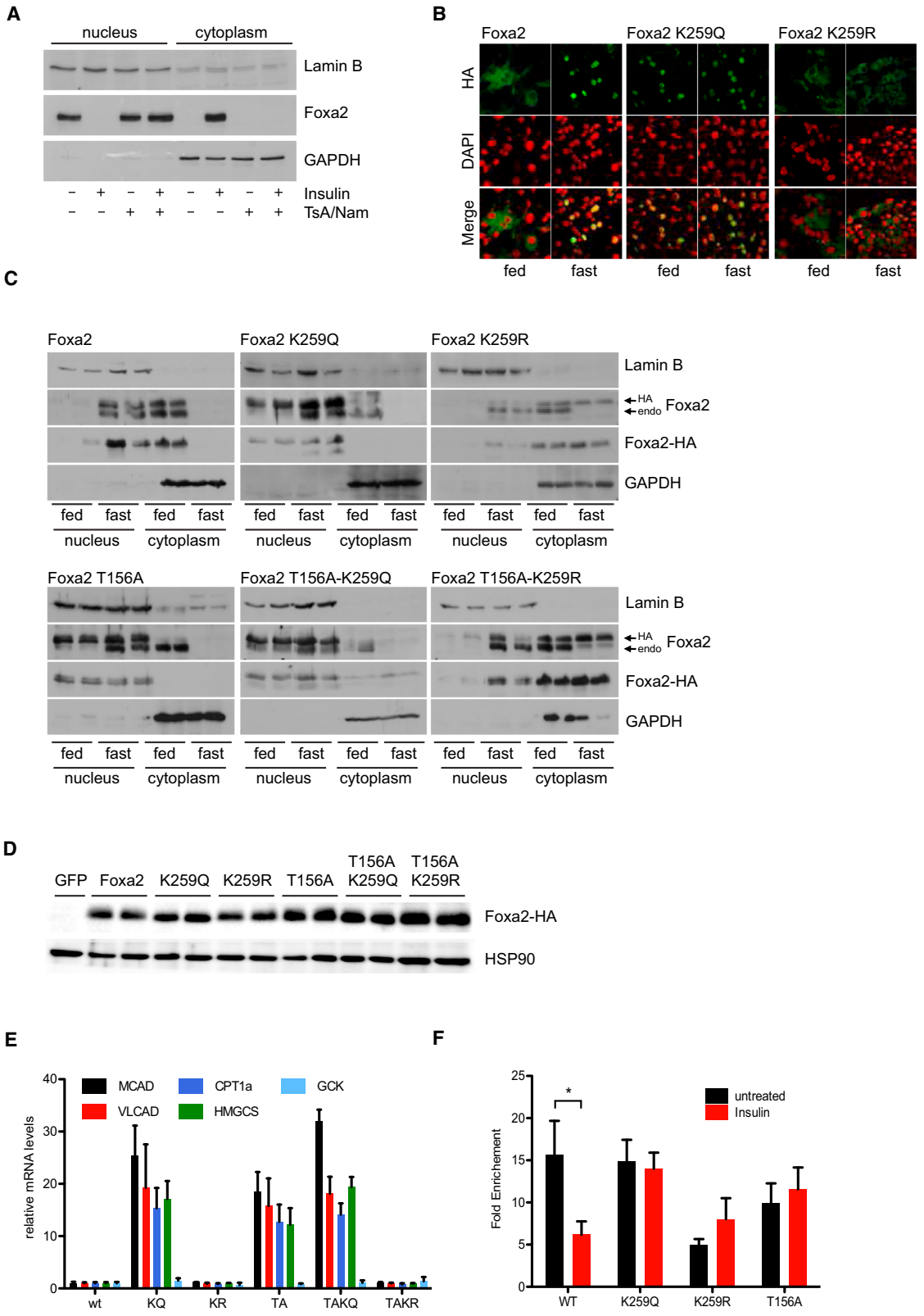

Figure 4. Acetylating Foxa2 Determines Its Localization and Activity

(A) Immunoblots showing cellular fractionation of Hepa1-6 cells, which have been serum-starved overnight and stimulated with 500 nM insulin for 15 min after 2 hr TsA/Nam treatment.

(legend continued on next page)

in β-oxidation and ketone body formation were upregulated in livers overexpressing K259Q, T156A, and T156A-K259Q mutants compared to livers expressing wild-type Foxa2 or K259R and T156A-K259R mutants (Figure 4E). These data indicate that acetylation at Lys259 not only determines subcellular localization but also regulates transcriptional activity of Foxa2. To determine whether DNA binding is affected in the different Foxa2 mutants, we performed chromatin immunoprecipitation (ChIP) analyses of the MCAD promoter in fasted and insulin-stimulated primary hepatocytes of *C57BL/6* mice infected with recombinant adenovirus expressing the indicated Foxa2 mutants (Figure 4F). Wild-type Foxa2 binding to Foxa2 sites in the MCAD promoter was decreased by insulin stimulation, while K259Q and T156A were bound to the promoter independent of insulin stimulation. The fold enrichment of K259R at the MCAD promoter was in all states comparable to the levels found in insulin-stimulated wild-type Foxa2 samples.

We next investigated whether hepatic expression of the Foxa2 mutants that lack or mimic acetylation states has an impact on liver metabolism and/or insulin tolerance in lean mice. Liver triglyceride levels, mitochondrial β-oxidation, and ketogenesis and plasma ketone body concentrations were similar in all groups (Figures S3B–S3E), and insulin tolerance, determined during an intraperitoneal insulin tolerance test, revealed no significant differences in the integrated glucose area under the curve (Figures S3F and S3G). These results indicate that transient overexpression of Foxa2 acetylation mutants does not affect glucose and lipid metabolism in chow-fed mice and are in agreement with earlier observations showing normal metabolism following adenoviral overexpression of constitutively active Foxa2-T156A in lean wild-type mice (Wolfrum et al., 2004).

Foxa2 K259 Is Constitutively Active in Hyperinsulinemic *ob/ob* Mice

Endogenous Foxa2 is permanently inactivated in high-fat diet and genetic obese mouse models by nuclear exclusion (Wolfrum et al., 2004; Silva et al., 2009) and therefore a good model to study the physiological effect of mutant Foxa2 proteins. For instance, we previously showed that Foxa2-T156A is able to restore Foxa2 activity, whereas wild-type Foxa2 is constitutively cytoplasmic and inactive in these hyperinsulinemic mice (Wolfrum et al., 2004). Using recombinant adenoviruses, we expressed wild-type Foxa2; single T156A, K259R, and K259Q; and double T156A-K259R and T156A-K259Q mutants in livers of *ob/ob* mice (Figure 5A). Nuclear and cytoplasmic extracts from liver of these mice showed that wild-type Foxa2, K259R, and T156A-K259R are constitutively cytoplasmic, whereas the T156A, K259Q, and T156A-K259Q Foxa2 proteins remained in the nucleus (Figure 5B). We next examined the activity of Lys259 mutants in these mice by measuring Foxa2 target gene expression using quantitative real-time PCR. Consistent with previous findings from ad libitum fed *C57BL/6* mice (Figure 4E), mRNA levels of target genes encoding for enzymes involved in mitochondrial β-oxidation and ketogenesis were not changed in livers overexpressing Foxa2, K259R, and T156A-K259R but were significantly upregulated in livers of T156A, K259Q, and T156A-K259Q injected hyperinsulinemic mice (Figure 5C). To further elucidate the physiological effect of the Lys259 mutants in *ob/ob* mice, we monitored plasma insulin concentration before and after adenoviral expression of Foxa2 mutants (Figure 5D). A significant decrease was observed in mice injected with adenovirus expressing T156A, K259Q, and T156A-K259Q Foxa2 mutants. This decrease correlated with increased levels of phosphorylation of key phosphoproteins of the insulin-signaling cascade in livers of mice injected with adenovirus expressing T156A and K259Q mutants (Figure 5E). Consistent with the gene expression data, we also observed no changes in ketone body production and fatty acid oxidation in isolated mitochondria from *ob/ob* mice that were infected with adenovirus expressing Foxa2, K259R, and T156A-K259R mutants. In contrast, mice injected with T156A, K259Q, and T156A-K259Q showed significant increases in fatty acid metabolism (Figures 5F and 5G). In addition, liver triglyceride concentrations revealed a similar trend, with decreases observed only in livers of mice expressing active T156A, K259Q, and T156A-K259Q (data not shown). Taken together, these results indicate that Foxa2 acetylation also increases the activity of Foxa2 in hyperinsulinemic, insulin-resistant mice.

Foxa2-K259Q Improves Hepatic Metabolism in *db/db* Mice

Obese *db/db* mice on the BKS background develop an extreme type 2 diabetes phenotype, with hyperglycemia, obesity, hepatic steatosis, and (in the beginning) elevated plasma insulin concentrations. We used this model to study the physiological and metabolic consequences of expressing Foxa2 acetylation mutants in the liver under extreme metabolic conditions. Adenoviral expression of T156A, K259Q, and T156A-K259Q mutants results in significant improvement of the initial hyperglycemia as soon as 2 days after injection (Figure 6A), without causing any body weight loss (Figure 6B). This effect was not observed in wild-type Foxa2-, K259R-, T156A-K259R-, GFP-, or PBS-injected animals, although hepatic Foxa2-HA expression levels were comparable between all Foxa2 mutants (Figure S4A). In addition, in T156A, K259Q, and T156A-K259Q animals, plasma insulin levels dropped more than 3-fold (Figure 6C), and insulin sensitivity, determined during an intraperitoneal insulin tolerance test, was significantly increased (Figures 6D and S4B) when compared to wild-type Foxa2-, PBS-, or GFP-injected animals.

(B–E) *C57BL/6* mice were injected with the indicated adenovirus expressing HA-tagged Foxa2. Livers of mice that were either fasted for 16 hr or fed ad libitum were analyzed by immunofluorescence microscopy (B) or cellular fractionation and immunoblotting (C). Ad libitum fed mice were additionally treated with 1 U/kg insulin 15 min prior to harvesting (B). Lamin B and Gapdh expression levels were used as the nuclear and cytosolic markers, respectively (C). Immunoblots showing the expression levels of hepatic Foxa2-HA are shown (D). Transcript levels of Foxa2 target genes were measured in livers of fed *C57BL/6* mice injected with recombinant adenovirus expressing the indicated Foxa2 mutants (E). The relative mRNA abundance of Foxa2 target genes was determined by qPCR. Values are normalized to 36B4 expression levels. MCAD, medium-chain acyl-CoA dehydrogenase; VLCAD, very-long-chain acyl-CoA dehydrogenase; CPT1a, carnitine palmitoyltransferase 1a; HMGCS, HMG CoA synthase.

(F) ChIP analysis of the MCAD promoter in fasted and insulin-stimulated primary hepatocytes from *C57BL/6* mice infected with recombinant adenovirus expressing the indicated Foxa2 mutants. Values are the mean ± SD; *$p < 0.05$; $n = 4$.

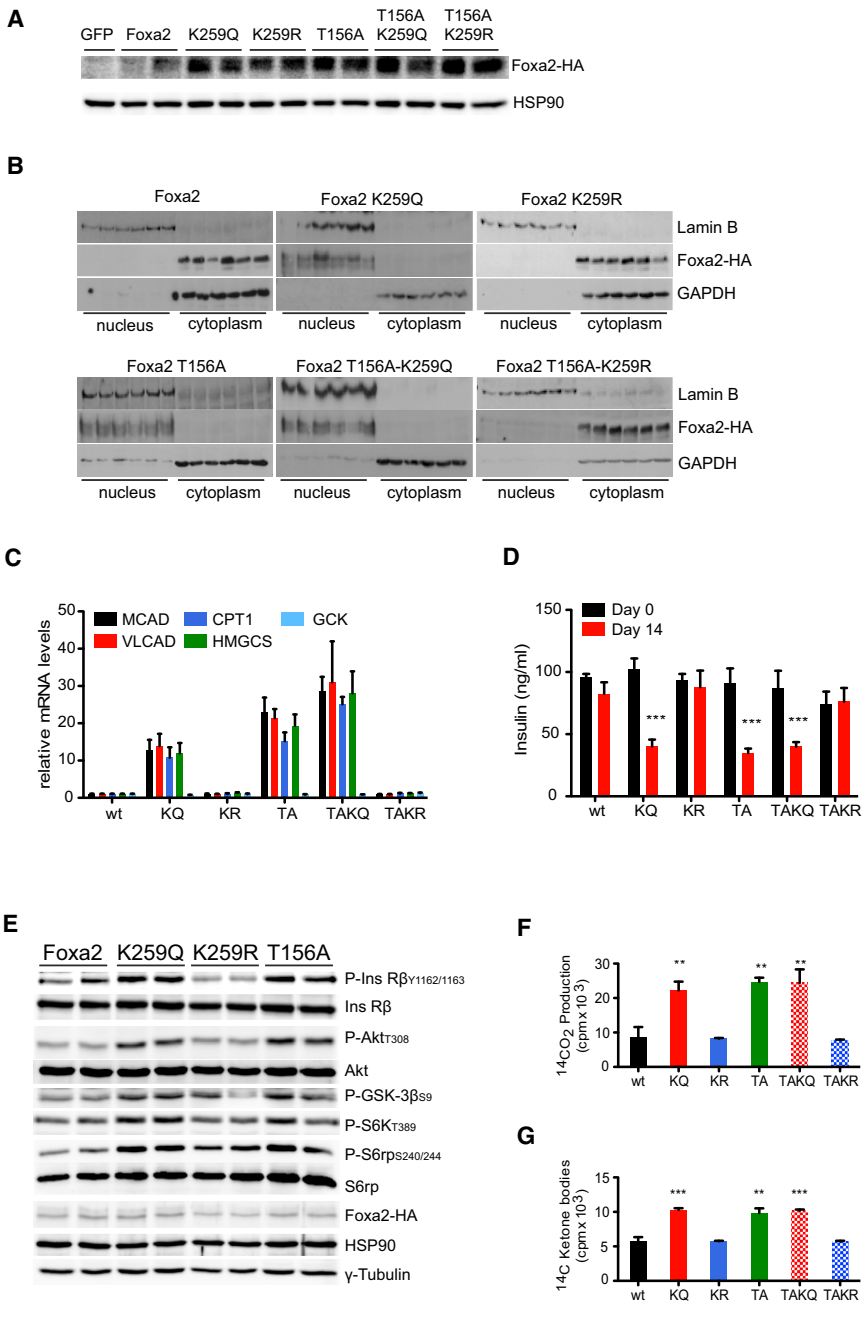

Figure 5. Foxa2-K259Q Is Active in Livers of Hyperinsulinemic *ob/ob* Mice

(A) Immunoblots showing the expression levels of Foxa2-HA.

(B) Immunoblots showing cellular fractionation of livers from *ob/ob* mice infected with adenovirus expressing HA-tagged Foxa2 mutants. Lamin B and Gapdh expression levels were used as nuclear and cytosolic markers, respectively.

(C–G) Transcript levels of Foxa2 target genes and metabolic parameters were measured in *ob/ob* mice injected with the indicated adenovirus. Shown are mean mRNA levels of Foxa2 target genes from liver (C), plasma insulin levels before and after adenovirus injection (D), and key phosphoproteins of the insulin-signaling cascade that were analyzed by western blotting (E). β-oxidation (F) and ketone body production (G) by liver mitochondria from *ob/ob* animals was measured by the formation of $^{14}CO_2$ and ^{14}C-labeled acid-soluble products, respectively, from ^{14}C-palmitic acid. Values are the mean ± SD; $^{**}p < 0.01$; $^{***}p < 0.001$; n = 5–6.

of *db/db* mice improved hyperglycemia, hepatic steatosis, and insulin sensitivity, whereas wild-type Foxa2, K259R, and T156A-K259R mutants had no effect on these parameters.

DISCUSSION

Foxa2 has been shown to be a key regulator of the transcriptional program of the liver in response to fasting and feeding (Wolfrum et al., 2004; Zhang et al., 2005). Earlier studies showed that Foxa2 is inactivated upon feeding or increased plasma insulin levels via insulin-PI3K-Akt signaling-mediated phosphorylation at Thr156 and nuclear exclusion (Wolfrum et al., 2003).

We have now identified a regulatory posttranslational modification (PTM) of Foxa2, namely acetylation at Lys259, catalyzed by the lysine acetyl transferase p300. Computational analysis (http://ds9.rockefeller.edu/basu/predmod.html) predicted Lys275 acetylation, which we could also experimentally confirm, but failed to identify Lys259 acetylation. Our subsequent studies focused on Lys259, since only this residue was also acetylated in the human liver cell line HepG2. A recent in silico study has also predicted several putative p300 acetylation sites on the homologous transcription factor Foxa1, among them Foxa1 Lys270, which corresponds to Lys259 in Foxa2. Acetylation assays with purified recombinant Foxa1 and p300 or the catalytic domain of p300 showed that Foxa1 can be acetylated in vitro and that the DNA binding potential of in vitro acetylated Foxa1 is diminished (Kohler and Cirillo, 2010). In contrast to our study, Kohler and Cirillo focused on Foxa1, which, albeit

Hepatic steatosis, quantified as total triglyceride content or in oil red O stainings on liver sections (Figures 6E and 6F), was markedly reduced in animals after T156A, K259Q, and T156A-K259Q expression. Consistent with these results, ketogenesis and mitochondrial β-oxidation were increased in livers of mice injected with Foxa2 T156A, K259Q, or T156A-K259Q (Figures 6G and S4C). We also found increased plasma ketone body concentrations in mice expressing Foxa2 T156A, K259Q, or T156A-K259Q (Figure 6H), while plasma triglyceride, nonesterified fatty acid (NEFA), and cholesterol levels were not significantly altered after Foxa2 mutant expression (Figures S4D–S4F). To summarize, expression of Foxa2-T156A, K259Q, and T156A-K259Q mutants in the liver

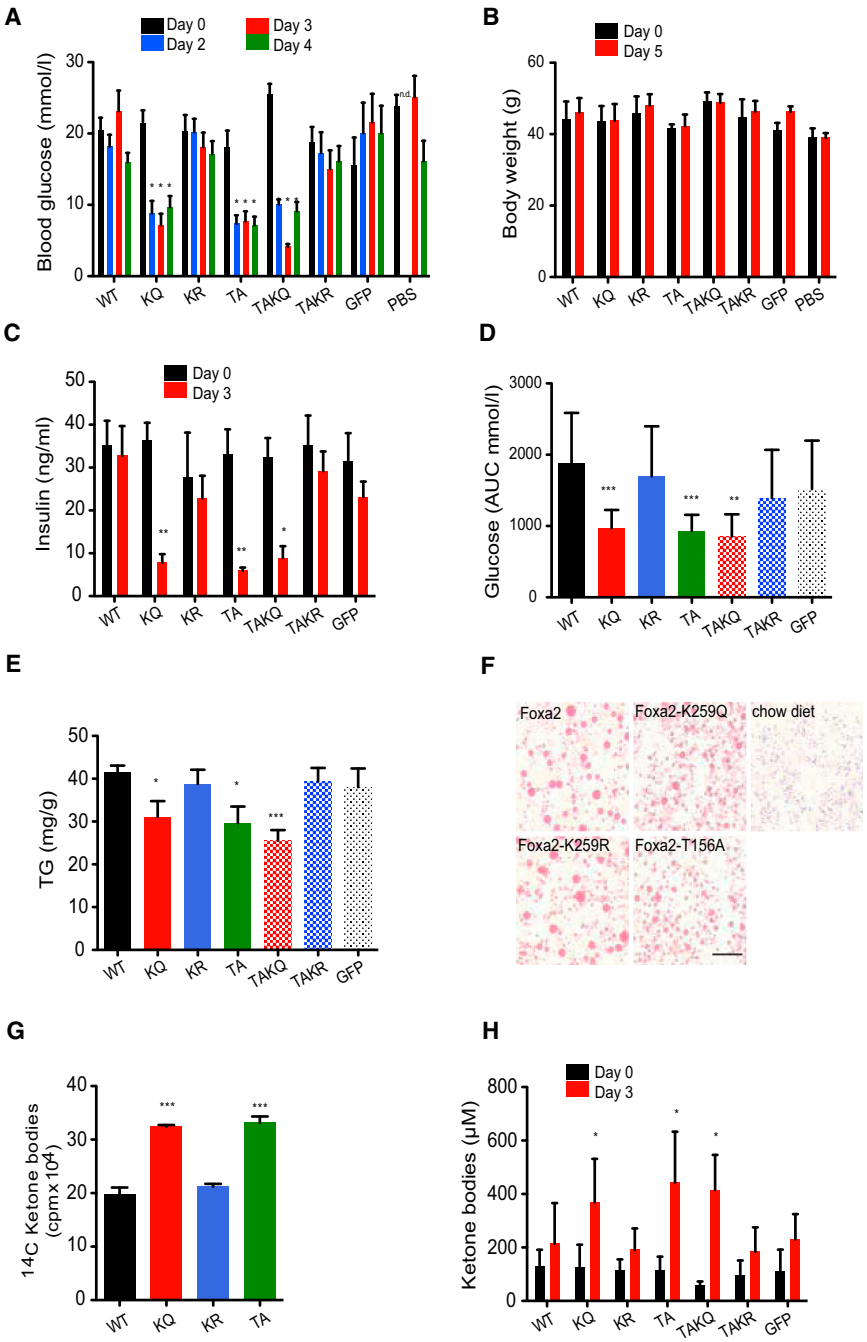

Figure 6. Foxa2-K259Q Is Active in Livers of Hyperinsulinemic *db/db* Mice

(A–H) Obese *db/db* (on a BKS background) mice were injected with recombinant adenovirus expressing the indicated Foxa2 mutants. Blood glucose levels (A), bodyweight (B), plasma insulin (C), and plasma ketone body concentrations (D) were measured before (day 0) and during the study. (E) Total liver triglyceride content was measured from 50 mg liver tissue. (F) Representative images of oil red O stainings of fixed liver sections from animals treated with the indicated adenovirus. (G) Insulin sensitivity was assayed during an intraperitoneal insulin tolerance test using 2 U/kg insulin. Areas under the curve (AUC) quantifications for glucose of averaged individual animals excluding the 15 min time point are shown. (H) Ketone body production by liver mitochondria from fasted animals was measured by the formation of ^{14}C-labeleld acid-soluble products from ^{14}C-oleic acid. Values ± SD; *$p < 0.05$; **$p < 0.01$; ***$p < 0.001$; $n \geq 4$. In (A), (C), and (E), values are the mean ± SEM; n = 6–17.

homologous to Foxa2, has different biological functions (Le Lay and Kaestner, 2010), and mainly used in vitro systems with overexpressed KATs, thereby forcing acetylation under nonphysiological conditions. Furthermore, we could not detect acetylation at any of the other predicted lysine residues in the winged helix domain, although the sequences are well conserved between Foxa1 and Foxa2 and were covered by our tandem MS analysis. In our study, we could show that acetylation of Foxa2 Lys259 is indeed catalyzed by p300 and demonstrate that both proteins also physically interact. Supporting our findings, earlier studies have demonstrated that Foxa2 and p300 are found in complexes (Rausa et al., 2003) and have synergistic effects at promoter sites (Liu et al., 2005; Qi et al., 2010). However, these studies did not report acetylation of Foxa2. Next, our results showed that deacetylation of Foxa2 is dependent on several HDACs, since inhibition of class I/II and III HDACs was necessary to detect increased Foxa2 acetylation. It has been reported that the 18 HDACs, which can be subdivided in four classes, show functional redundancy (Haberland et al., 2009), for instance in deacetylating lysine residues of NF-κB (Spange et al., 2009). Knockdown of Sirt1, belonging to HDAC class III and physically interacting with Foxa2, in combination with class I/II inhibition was sufficient to prevent Foxa2 deacetylation, proving an involvement of Sirt1 to be the responsible HDAC class III for Foxa2 in the regulation of Foxa2 acetylation. The class I/II HDACs responsible for deacetylation of Foxa2 are currently unknown. Their relative contribution on Foxa2 acetylation and activity as well as their regulation by endogenous and external factors will be important to study in the future.

Next we could demonstrate that glucagon promotes acetylation of Foxa2 Lys259. The notion that glucagon increases the activity of Foxa2 is in agreement with the known role of the pancreatic hormone in many metabolic pathways, besides its function as a regulator of glucose homeostasis (Habegger et al., 2010). It was shown that either prolonged fasting or glucagon treatment stimulated the rate of hepatic fatty acid oxidation and the expression of genes involved in β-oxidation, such as CPT1α or MCAD, in wild-type but not in glucagon

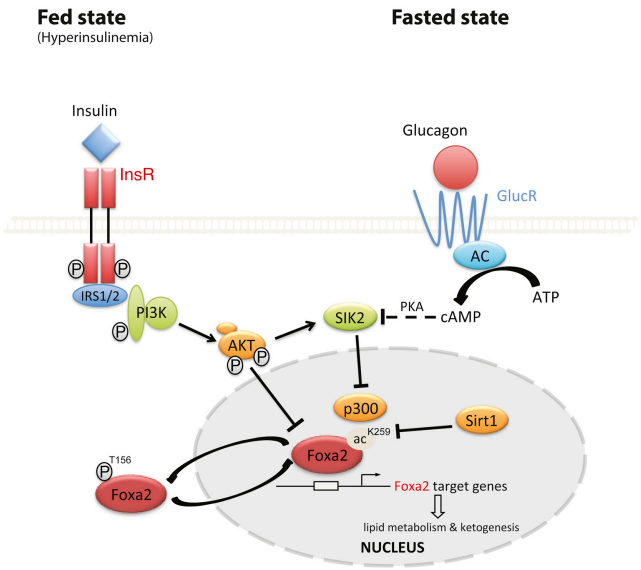

Figure 7. Model for Regulation of Foxa2 Activity by Insulin and Glucagon Signaling in Fed and Fasted States, Respectively

Schematic representation illustrating the regulation of Foxa2 and its target genes in hepatic lipid metabolism and ketogenesis. After feeding, insulin signaling leads to the inactivation of Foxa2 through phosphorylation of Thr156, nuclear exclusion, thereby resulting in inhibition of Foxa2 target gene expression and reduced hepatic lipid metabolism and gluconeogenesis. During fasting, plasma insulin levels decrease and glucagon levels rise. Glucagon signaling activates the adenylate cyclase (AC), leading to inhibition of SIK2, a negative regulator of p300 activity. Acetylation of Foxa2 Lys259 by p300 increases its transcriptional activity. Sirt1 can inactivate Foxa2 by deacetylation and can thereby fine-tune the activity of Foxa2.

receptor knockout mice (Longuet et al., 2008). At the same time, glucagon receptor knockout mice were more susceptible to developing a hepatic steatosis. The mentioned genes are well-known target genes of Foxa2, and reactivation of Foxa2 in the liver can improve hepatic steatosis in *ob/ob* or *db/db* mice, as shown in this study and before (Wolfrum et al., 2004). The role of glucagon in the regulation of hepatic ketogenesis was also investigated in several studies. It was shown that suppression of glucagon secretion by somatostatin prevented the development of ketoacidosis in type 1 diabetic patients (Gerich et al., 1975). In isolated hepatocytes, increases in the rate of ketogenesis and β-oxidation could be observed after glucagon stimulation, whereas insulin had the opposite effect (Pégorier et al., 1989). These results could also be reproduced in primary human hepatocytes (Vons et al., 1991) and match the consequences of Foxa2 activity in the liver, which has been shown to be also a driver of the transcriptional program of ketogenesis (Wolfrum et al., 2004). Another recent study revealed that histone H4 acetylation and p300 occupancy at promoters of CPT1α and HMGCS2, both also Foxa2 target genes, is increased during fasting (Sengupta et al., 2010). As shown in our study, p300 physically interacts with Foxa2. Thus, PPARα and Foxa2, which have additive transcriptional activity at the same promoter (Wolfrum and Stoffel, 2006), might confer the increased transcriptional activity through p300. Montminy and colleagues showed that salt-inducible kinase 2 (SIK2) is able to phosphorylate p300 at Ser89 (Liu et al., 2008), a phosphorylation that has been reported to inhibit p300 transcriptional activity (Yuan and Gambee, 2000). Upon insulin stimulation p300 Ser89 phosphorylation was increased, whereas glucagon decreased it. We could verify the effect of glucagon stimulation on p300 Ser89 phosphorylation, which also resulted in increased Foxa2 Lys259 acetylation. Based on these results, we propose a model in which Foxa2 is inactivated by insulin during fed states and (re-) activated by glucagon upon fasting (Figure 7). Finally, glucagon has been implicated in the regulation of energy expenditure and food intake. Earlier studies have shown that oxygen consumption in rats was increased after glucagon infusion (Davidson et al., 1957), and in human studies it could be shown that a pharmacological dose of glucagon increased resting energy expenditure (Nair, 1987). Additional studies revealed that glucagon decreases food intake due to increased satiation (Martin and Novin, 1977; Le Sauter and Geary, 1991). Recently it was suggested that the inhibitory effect of glucagon on food intake is partially mediated through direct actions in the brain (Kurose et al., 2009). It will be interesting to see whether acetylation and activity of Foxa2 in the central nervous system is also regulated by glucagon. Foxa2 has been shown to be involved in the regulation of food intake. In particular Foxa2 regulates the expression of the orexigenic neuropeptides MCH and orexin in the lateral hypothalamus (Silva et al., 2009).

The metabolic and physiological consequences of Foxa2 Lys259 acetylation were studied in several mouse models, including lean, obese, and diabetic animals. A Foxa2 mutant mimicking acetylated Lys259 was transcriptionally active and nuclear, independent of the nutritional or physiological state of the mice. As a consequence, hepatic expression of this mutant was able to improve the metabolic phenotype of *ob/ob* and *db/db* mice. In particular, hyperinsulinemia, hyperglycemia, and hepatic steatosis were significantly improved, comparable to levels observed with the constitutively active Foxa2 mutant T156A. In contrast, the acetylation-deficient Lys259 mutant was inactive and predominantly cytoplasmic and had no metabolic beneficial effects when expressed in livers of obese or diabetic animals. In addition, the Foxa2 double mutant K259R-T156A was also inactive, suggesting a hierarchical regulation of Foxa2 by PTMs regarding its subcellular localization and activity and indicating that the effect of Lys259 acetylation is dominant over Thr156 phosphorylation. Sirt1, one of the HDACs involved in Foxa2 Lys259 deacetylation is a major regulator of cellular energy homeostasis (Houtkooper et al., 2012), but its function in the liver is still controversial. Several studies have assessed the role of Sirt1 in the liver and found that Sirt1 can either inhibit or enhance hepatic glucose production through interacting with different proteins under different physiological conditions (Rodgers et al., 2005; Banks et al., 2008; Liu et al., 2008; Erion et al., 2009; Wei et al., 2011), and it has also been reported that Sirt1 loss accelerates or protects against hepatic steatosis (Chen et al., 2008; Purushotham et al., 2009). Also, the notion that Sirt1 activity is increased by caloric restriction (Cohen et al., 2004) has been challenged (Chen et al., 2008). Our study revealed that, in addition to Sirt1, other HDACs also deacetylate Foxa2, and this process might be regulated by the physiological and metabolic state. It will be important to study the regulatory network of HDACs and their regulation by signaling pathways with respect to Foxa2 activity.

EXPERIMENTAL PROCEDURES

Materials

Human recombinant insulin, glucagon, forskolin, nicotinamide and trichostatin A were purchased from Sigma-Aldrich. Antibodies for HA, Foxa2, P-IRβ, IRβ, HSP90, γ-tubulin, p300, GCN5, and lamin B were from Santa Cruz; GAPDH was from Abcam; and Sirt1 was from Sigma. Ac-Lys, P-Akt, Akt, P-GSK3α/β, P-S6K, P-Creb, Creb, P-S6rp, S6rp, HDAC3, HDAC5, HDAC7, and SRC-1 antibodies were purchased from Cell Signaling. Polyclonal antiacetylated Foxa2 (Lys259) was generated by immunizing rabbits with a synthetic acetylated peptide corresponding to the residues −10 and +10 surrounding Lys259 of Foxa2. Antibodies were purified by peptide affinity chromatography (21st Century Biochemicals).

Plasmids

HA-FLAG-tagged Foxa2 wild-type and mutants were in pcDNA3 expression vectors as previously described (Wolfrum et al., 2003). Lys259 and Lys275 constructs were generated by site-directed mutagenesis, and the sequences were confirmed by sequencing. The following additional expression vectors were used: p300 (Addgene plasmid 10718), p300Δ33 (Addgene plasmid 10719), PCAF (Addgene plasmid 8941), and SRC-1, Tip60, and GCN5 (kindly provided by Pere Puigserver).

Recombinant Adenoviruses

Adenoviruses were generated using the Rapid Adenovirus Production System (ViraQuest Inc.). GFP was coexpressed from an independent promoter in addition to HA-tagged Foxa2. Ad-GFP, Ad-Foxa2, and Ad-T156A were described previously (Wolfrum et al., 2004). For in vivo experiments, mice were injected through the tail vein with 8×10^8 plaque-forming units (pfu) of adenovirus in 200 μl PBS. Empty virus expressing only GFP served as control (Ad-GFP).

Animal Models

All animals studied were 8- to 12-week-old male C57BL/6, *ob/ob*, or *db/db* mice, purchased from Charles River and maintained on a normal chow diet and a 12 hr light/dark cycle in a pathogen-free animal facility. All animal studies were approved by the Ethics committee of the Kantonale Veterinäramt Zürich.

Cell Lines and Primary Hepatocytes

HepG2 cells were maintained as described before (Howell and Stoffel, 2009). Hepa1-6 cells were maintained in DMEM (4.5 g/l glucose, 110 mg/l pyruvate, 4 mM L-glutamine, 100 U/ml Pen/Strep) supplemented with 10% fetal bovine serum (Sigma). Serum starvation was carried out for 16 hr in DMEM without FBS and Pen/Strep. Primary hepatocytes were isolated as previously described (Wolfrum et al., 2004) and maintained in DMEM (1 g/l glucose, 110 mg/l pyruvate, 4 mM L-glutamine, 100 U/ml Pen/Strep). All cells were cultured in a humidified incubator at 37°C and 5% CO_2.

Nuclear/Cytosolic Extracts

Hepa1-6 cells were grown to 80% confluency and serum-starved for 18 hr, followed by the indicated treatments (TsA/Nam: 2 hr with 5 μM TsA and 5 mM Nam; insulin: 500 nM human recombinant insulin for 15 min at 37°C). Nuclear and cytoplasmic extracts were prepared as previously described (Howell and Stoffel, 2009). Briefly, cells were swollen on ice in hypotonic lysis buffer (10 mM HEPES [pH 7.9], 1.5 mM $MgCl_2$, 10 mM KCl) containing DTT, TsA, Nam, and protease inhibitors (Complete mixture, Roche Applied Science) and permeabilized by the addition of NP40 to 0.6%. After centrifugation at 10,400 × *g* for 30 s at 4°C, the supernatants (cytoplasmic extracts) were collected, and nuclear pellets were resuspended in nuclear lysis buffer (10 mM HEPES [pH 7.9], 100 mM KCl, 3 mM $MgCl_2$, 0.1 mM EDTA) containing DTT, TsA, Nam, and protease inhibitors. Nuclei were lysed by the gradual addition of one-tenth volume of 4M $(NH_4)_2SO_4$ over 30 min. For liver experiments, ~50 mg of liver was dounced in ice-cold hypotonic lysis buffer 10 times with a tight piston.

Whole-Cell Lysis and Immunoblotting

For whole-cell lysis, cells were washed with ice-cold PBS and dissolved in lysis buffer (1% Triton X-100, 50 mM Tris [pH 7.5], 300 mM NaCl, 1 mM EGTA, 1 mM EDTA, 0.1% SDS) containing TsA, Nam, protease (Complete mixture, Roche Applied Science), and phosphatase inhibitors (Halt Phosphatase Inhibitor Cocktail, Pierce). Equal amounts of cell lysates were separated on SDS-PAGE and blotted onto a nitrocellulose membrane (Immobilon). Proteins were detected by immunoblotting with ECL detection. For liver experiments, ~50 mg of liver was processed with a TissueLyser (QIAGEN) directly in whole-cell lysis buffer.

Immunoprecipitation

HA-tagged Foxa2 were immunoprecipitated from whole-cell lysates using anti-HA-Agarose (Sigma) or polyclonal anti-Foxa2 antibodies for 1 hr at 4°C. TsA, Nam, protease, and phosphatase inhibitors were added to all buffers. Proteins were eluted with SDS-loading buffer and separated by SDS-PAGE.

Immunofluorescence Microscopy

Liver pieces were frozen directly in OCT at −80°C. Sections were cut on a cryotome at 8–10 μm thickness, fixed in 4% PFA (in PBS) for 7 min, and frozen again. Slides were thawed, washed three times for 5 min in PBS, permeabilized for 10 min with 0.3% Triton X-100 in PBS, rinsed with PBS, and blocked for 1 hr at room temperature in PBS 0.025% Triton X-100, 1% BSA, and 5% goat serum. Slides were incubated overnight at 4°C in PBS 0.025% Triton X-100, 1% BSA, and 5% goat serum with 1:50 HA.11 Clone 16B12 Monoclonal Antibody, Alexa Fluor Labeled (Covance A594-101L). Slides were then washed three times for 15 min with 0.025% Triton X-100 in PBS and mounted with DAPI (H-1200 Reactolab). Images were scanned on a Leica Confocal TCS SPE at 40×.

Oil Red O Staining

Frozen sections (7 μm) from OCT-embedded, snap-frozen liver tissues were fixed with 5% formalin, washed once in 60% isopropanol, and stained with 0.5% oil red O in propylene glycerol for 1 hr at room temperature. Sections were washed with isopropanol and mounted.

Gene Expression

RNA was isolated from 20 mg of liver tissue using an RNA extraction kit (Sigma) and treated with DNase I (Sigma). Five milligrams of total RNA was used for first-strand cDNA synthesis using SuperScript III RT and hexamer primers (Invitrogen). PCR products were measured as a function of SYBR Green incorporation using LightCycler 480 SYBR Green I Master mix (Roche) and the Mx3005P Real-Time QPCR Detection System (Stratagene). Values shown are given in arbitrary units based on a standard curve and normalized to 36B4.

Transfection and RNA Interference

Hepa1-6 cells and primary hepatocytes were transfected using Lipofectamine 2000 (Invitrogen) according to the manufacturer's instructions. For gene-silencing experiments, cells were transfected with 50 nM siRNA using Lipofectamine RNAiMAX (Invitrogen) following a forward transfection protocol. Cells were harvested 48 or 72 hr posttransfection. siRNAs were purchased from Dharmacon (Smart Pools).

Physiological and Metabolic Measurements

Blood glucose was measured using a standard glucometer (Ascensia Contour, Bayer). Ketone bodies and free fatty acids were measured by a colorimetric assay system (Wako Chemicals); cholesterol and triglycerides were determined by a colorimetric assay system (Roche). Plasma insulin levels were measured with the Sensitive Rat Insulin RIA kit (Linco Research). Liver triglycerides were extracted by the Folch method (Folch et al., 1957) and quantified by colorimetric assay (Roche). For the insulin tolerance test, mice were intraperitoneally injected with 0.54 U/kg or 2 U/kg of human recombinant insulin, and blood glucose was monitored over 120 min. Area under the curve was calculated excluding the 15 min time points.

Mitochondrial β-Oxidation and Ketone Body Formation

Mitochondria were isolated from 200 mg of PBS-perfused mouse livers by differential centrifugation, as previously described (Hoppel et al., 1979). β-oxidation of [1-^{14}C]palmitic acid or [1-^{14}C]oleic acid by liver mitochondria in samples normalized to mitochondrial protein was determined as described (Fréneaux et al., 1988). CO_2 trapped on NaOH moistened filter papers was determined by measuring ^{14}C radiation in a scintillation counter. Ketone

body formation was assayed in the supernatant of the incubation mixture after centrifugation at 4,000 × *g* for 10 min. ^{14}C acid-soluble products of mitochondrial β-oxidation were counted from an aliquot of the supernatant.

Chromatin Immunoprecipitation

Chromatin immunoprecipitation (ChIP) was performed as described (Nelson et al., 2006). Details are given in the Supplemental Experimental Procedures.

Mass Spectrometry

MS analyses are described in detail in the Supplemental Experimental Procedures.

Statistical Analysis

Statistics were determined using the unpaired Student's t test with Prism software. Data are calculated as the mean ± SD unless otherwise indicated. Statistical significance is represented in figures by *, $p \leq 0.05$; **, $p \leq 0.01$; ***, $p \leq 0.001$.

SUPPLEMENTAL INFORMATION

Supplemental Information includes four figures, one table, and Supplemental Experimental Procedures and can be found with this article online at http://dx.doi.org/10.1016/j.cmet.2013.01.014.

ACKNOWLEDGMENTS

We thank Christian Wolfrum for helpful discussion and Bianca Kaps, Michèle Müller, and Regina Kubsch for technical support. We would also like to thank Pere Puigserver for providing plasmids, Frank Gillardon (Bohringer-Ingelheim) for providing reagents, and Johan Auwerx for the Sirt1$^{fl/fl}$ mice. We acknowledge salary support from an EMBO LTF (to T.P.). This work was funded in part by the SNSF, grant number 310030_141209 (to M.S.).

Received: June 6, 2011
Revised: November 29, 2012
Accepted: January 23, 2013
Published: February 14, 2013

REFERENCES

Altarejos, J.Y., and Montminy, M. (2011). CREB and the CRTC co-activators: sensors for hormonal and metabolic signals. Nat. Rev. Mol. Cell Biol. *12*, 141–151.

Banerjee, A., Meyer, K., Mazumdar, B., Ray, R.B., and Ray, R. (2010). Hepatitis C virus differentially modulates activation of forkhead transcription factors and insulin-induced metabolic gene expression. J. Virol. *84*, 5936–5946.

Banks, A.S., Kon, N., Knight, C., Matsumoto, M., Gutiérrez-Juárez, R., Rossetti, L., Gu, W., and Accili, D. (2008). SirT1 gain of function increases energy efficiency and prevents diabetes in mice. Cell Metab. *8*, 333–341.

Bochkis, I.M., Rubins, N.E., White, P., Furth, E.E., Friedman, J.R., and Kaestner, K.H. (2008). Hepatocyte-specific ablation of Foxa2 alters bile acid homeostasis and results in endoplasmic reticulum stress. Nat. Med. *14*, 828–836.

Chen, D., Bruno, J., Easlon, E., Lin, S.-J., Cheng, H.-L., Alt, F.W., and Guarente, L. (2008). Tissue-specific regulation of SIRT1 by calorie restriction. Genes Dev. *22*, 1753–1757.

Cohen, H.Y., Miller, C., Bitterman, K.J., Wall, N.R., Hekking, B., Kessler, B., Howitz, K.T., Gorospe, M., de Cabo, R., and Sinclair, D.A. (2004). Calorie restriction promotes mammalian cell survival by inducing the SIRT1 deacetylase. Science *305*, 390–392.

Davidson, I.W., Salter, J.M., and Best, C.H. (1957). Calorigenic action of glucagon. Nature *180*, 1124.

Erion, D.M., Yonemitsu, S., Nie, Y., Nagai, Y., Gillum, M.P., Hsiao, J.J., Iwasaki, T., Stark, R., Weismann, D., Yu, X.X., et al. (2009). SirT1 knockdown in liver decreases basal hepatic glucose production and increases hepatic insulin responsiveness in diabetic rats. Proc. Natl. Acad. Sci. USA *106*, 11288–11293.

Folch, J., Lees, M., and Sloane Stanley, G.H. (1957). A simple method for the isolation and purification of total lipides from animal tissues. J. Biol. Chem. *226*, 497–509.

Fréneaux, E., Labbe, G., Letteron, P., Dinh, T.L., Degott, C., Genève, J., Larrey, D., Pessayre, D., and Pessayre, D. (1988). Inhibition of the mitochondrial oxidation of fatty acids by tetracycline in mice and in man: possible role in microvesicular steatosis induced by this antibiotic. Hepatology *8*, 1056–1062.

Gerich, J.E., Lorenzi, M., Bier, D.M., Schneider, V., Tsalikian, E., Karam, J.H., and Forsham, P.H. (1975). Prevention of human diabetic ketoacidosis by somatostatin. Evidence for an essential role of glucagon. N. Engl. J. Med. *292*, 985–989.

Habegger, K.M., Heppner, K.M., Geary, N., Bartness, T.J., DiMarchi, R., and Tschöp, M.H. (2010). The metabolic actions of glucagon revisited. Nat. Rev. Endocrinol. *6*, 689–697.

Haberland, M., Montgomery, R.L., and Olson, E.N. (2009). The many roles of histone deacetylases in development and physiology: implications for disease and therapy. Nat. Rev. Genet. *10*, 32–42.

Hoppel, C., DiMarco, J.P., and Tandler, B. (1979). Riboflavin and rat hepatic cell structure and function. Mitochondrial oxidative metabolism in deficiency states. J. Biol. Chem. *254*, 4164–4170.

Houtkooper, R.H., Pirinen, E., and Auwerx, J. (2012). Sirtuins as regulators of metabolism and healthspan. Nat. Rev. Mol. Cell Biol. *13*, 225–238.

Howell, J.J., and Stoffel, M. (2009). Nuclear export-independent inhibition of Foxa2 by insulin. J. Biol. Chem. *284*, 24816–24824.

Kahn, S.E., Hull, R.L., and Utzschneider, K.M. (2006). Mechanisms linking obesity to insulin resistance and type 2 diabetes. Nature *444*, 840–846.

Kohler, S., and Cirillo, L.A. (2010). Stable chromatin binding prevents FoxA acetylation, preserving FoxA chromatin remodeling. J. Biol. Chem. *285*, 464–472.

Koo, S.-H., Flechner, L., Qi, L., Zhang, X., Screaton, R.A., Jeffries, S., Hedrick, S., Xu, W., Boussouar, F., Brindle, P., et al. (2005). The CREB coactivator TORC2 is a key regulator of fasting glucose metabolism. Nature *437*, 1109–1111.

Kurose, Y., Kamisoyama, H., Honda, K., Azuma, Y., Sugahara, K., Hasegawa, S., and Kobayashi, S. (2009). Effects of central administration of glucagon on feed intake and endocrine responses in sheep. Anim. Sci. J. *80*, 686–690.

Le Lay, J., and Kaestner, K.H. (2010). The Fox genes in the liver: from organogenesis to functional integration. Physiol. Rev. *90*, 1–22.

Le Sauter, J., and Geary, N. (1991). Hepatic portal glucagon infusion decreases spontaneous meal size in rats. Am. J. Physiol. *261*, R154–R161.

Lin, H.V., and Accili, D. (2011). Hormonal regulation of hepatic glucose production in health and disease. Cell Metab. *14*, 9–19.

Liu, Y.-N., Lee, W.-W., Wang, C.-Y., Chao, T.-H., Chen, Y., and Chen, J.H. (2005). Regulatory mechanisms controlling human E-cadherin gene expression. Oncogene *24*, 8277–8290.

Liu, Y., Dentin, R., Chen, D., Hedrick, S., Ravnskjaer, K., Schenk, S., Milne, J., Meyers, D.J., Cole, P., Yates, J., 3rd., et al. (2008). A fasting inducible switch modulates gluconeogenesis via activator/coactivator exchange. Nature *456*, 269–273.

Longuet, C., Sinclair, E.M., Maida, A., Baggio, L.L., Maziarz, M., Charron, M.J., and Drucker, D.J. (2008). The glucagon receptor is required for the adaptive metabolic response to fasting. Cell Metab. *8*, 359–371.

Martin, J.R., and Novin, D. (1977). Decreased feeding in rats following hepatic-portal infusion of glucagon. Physiol. Behav. *19*, 461–466.

Nair, K.S. (1987). Hyperglucagonemia increases resting metabolic rate in man during insulin deficiency. J. Clin. Endocrinol. Metab. *64*, 896–901.

Nelson, J.D., Denisenko, O., and Bomsztyk, K. (2006). Protocol for the fast chromatin immunoprecipitation (ChIP) method. Nat. Protoc. *1*, 179–185.

Pandey, A.K., Bhardwaj, V., and Datta, M. (2009). Tumour necrosis factor-alpha attenuates insulin action on phosphoenolpyruvate carboxykinase gene

expression and gluconeogenesis by altering the cellular localization of Foxa2 in HepG2 cells. FEBS J. *276*, 3757–3769.

Pégorier, J.P., Garcia-Garcia, M.V., Prip-Buus, C., Duée, P.H., Kohl, C., and Girard, J. (1989). Induction of ketogenesis and fatty acid oxidation by glucagon and cyclic AMP in cultured hepatocytes from rabbit fetuses. Evidence for a decreased sensitivity of carnitine palmitoyltransferase I to malonyl-CoA inhibition after glucagon or cyclic AMP treatment. Biochem. J. *264*, 93–100.

Purushotham, A., Schug, T.T., Xu, Q., Surapureddi, S., Guo, X., and Li, X. (2009). Hepatocyte-specific deletion of SIRT1 alters fatty acid metabolism and results in hepatic steatosis and inflammation. Cell Metab. *9*, 327–338.

Qi, J., Nakayama, K., Cardiff, R.D., Borowsky, A.D., Kaul, K., Williams, R., Krajewski, S., Mercola, D., Carpenter, P.M., Bowtell, D., and Ronai, Z.A. (2010). Siah2-dependent concerted activity of HIF and FoxA2 regulates formation of neuroendocrine phenotype and neuroendocrine prostate tumors. Cancer Cell *18*, 23–38.

Rausa, F.M., Tan, Y., and Costa, R.H. (2003). Association between hepatocyte nuclear factor 6 (HNF-6) and FoxA2 DNA binding domains stimulates FoxA2 transcriptional activity but inhibits HNF-6 DNA binding. Mol. Cell. Biol. *23*, 437–449.

Rodgers, J.T., Lerin, C., Haas, W., Gygi, S.P., Spiegelman, B.M., and Puigserver, P. (2005). Nutrient control of glucose homeostasis through a complex of PGC-1alpha and SIRT1. Nature *434*, 113–118.

Saltiel, A.R., and Kahn, C.R. (2001). Insulin signalling and the regulation of glucose and lipid metabolism. Nature *414*, 799–806.

Sengupta, S., Peterson, T.R., Laplante, M., Oh, S., and Sabatini, D.M. (2010). mTORC1 controls fasting-induced ketogenesis and its modulation by ageing. Nature *468*, 1100–1104.

Silva, J.P., von Meyenn, F., Howell, J., Thorens, B., Wolfrum, C., and Stoffel, M. (2009). Regulation of adaptive behaviour during fasting by hypothalamic Foxa2. Nature *462*, 646–650.

Spange, S., Wagner, T., Heinzel, T., and Krämer, O.H. (2009). Acetylation of non-histone proteins modulates cellular signalling at multiple levels. Int. J. Biochem. Cell Biol. *41*, 185–198.

Vons, C., Pégorier, J.P., Girard, J., Kohl, C., Ivanov, M.A., and Franco, D. (1991). Regulation of fatty-acid metabolism by pancreatic hormones in cultured human hepatocytes. Hepatology *13*, 1126–1130.

Wei, D., Tao, R., Zhang, Y., White, M.F., and Dong, X.C. (2011). Feedback regulation of hepatic gluconeogenesis through modulation of SHP/Nr0b2 gene expression by Sirt1 and FoxO1. Am. J. Physiol. Endocrinol. Metab. *300*, E312–E320.

Wolfrum, C., and Stoffel, M. (2006). Coactivation of Foxa2 through Pgc-1β promotes liver fatty acid oxidation and triglyceride/VLDL secretion. Cell Metab. *3*, 99–110.

Wolfrum, C., Besser, D., Luca, E., and Stoffel, M. (2003). Insulin regulates the activity of forkhead transcription factor Hnf-3beta/Foxa-2 by Akt-mediated phosphorylation and nuclear/cytosolic localization. Proc. Natl. Acad. Sci. USA *100*, 11624–11629.

Wolfrum, C., Asilmaz, E., Luca, E., Friedman, J.M., and Stoffel, M. (2004). Foxa2 regulates lipid metabolism and ketogenesis in the liver during fasting and in diabetes. Nature *432*, 1027–1032.

Yuan, L.W., and Gambee, J.E. (2000). Phosphorylation of p300 at serine 89 by protein kinase C. J. Biol. Chem. *275*, 40946–40951.

Zhang, L., Rubins, N.E., Ahima, R.S., Greenbaum, L.E., and Kaestner, K.H. (2005). Foxa2 integrates the transcriptional response of the hepatocyte to fasting. Cell Metab. *2*, 141–148.